37th Cement and Concrete Science Conference
11-12 September 2017
University College London

Analysis of pore structure development of alkali-activated slag cement at early age

Xiaohong ZHU, Kai YANG, Zhilu ZHANG, Qing LI, Linwen YU, Changhui YANG,
College of Materials Science and Engineering, Chongqing University, Chongqing, China

Muhammed BASHEER
School of Civil Engineering, University of Leeds, Leeds, UK

Yaocheng WANG
School of Civil Engineering, Shenzhen University, Shenzhen, China

Song Mu
State Key Laboratory of High Performance Civil Engineering Materials, Jiangsu Sobute New Materials Co., Ltd, Nanjing, China

ABSTRACT

This study describes the results of a laboratory study dealing with changes in pore structure of AASC at early age. In order to achieve this, porosity, electrical conductivity of pore solution, electrical resistivity of hardened paste samples were determined and these data were further analysed to estimate tortuosity. Water absorption tests were also carried out to verify conclusions derived from the indirect method. Two AASCs with 0.35 and 0.5 liquid/solid ratios were tested at the age of 3, 7, 14 and 28 days along with pure Portland cement (PC) pastes for a purpose of comparison. The results show that the value of tortuosity decreases as the age increases, and for a given liquid/solid ratio, electrical resistivity and capillary porosity of AASC are lower than PC system, while an opposite trend is found for pore solution conductivity due to significantly higher ion concentration in AASC. More importantly, capillary pores in AASC are less tortuous than PC. In order to achieve comparable tortuosity as PC pore network, AASC needs to be cured for a longer duration.

1. INTRODUCTION

Alkali-activated slag cement (AASC) is a clinker-free binder comprising ground granulated blast furnace slag (GGBFS) sourced from metallurgical industries. It offers a range of high performance characteristics not easily achieved by PC, e.g. excellent mechanical strength and resistance to acid and sulphate attack [1,2]. Numerous applications have been reported to use this material in real application. However, it is established that chemical reaction kinetics and hydration products differ between AASC and PC [1,3], calling into question the suitability of using established PC-based material quality assessment methods for AASC-based products. An issue requiring clarification is minimum curing durations required for AASC systems in order to obtain comparable pore structures to PC-based materials. To address this, it is essential to examine and compare differences in the development of pore structure between AASC and PC systems, as an understanding of microstructural variations such as porosity, pore size distribution and pore tortuosity is key to optimising durability characteristics.

While numerous studies have been carried out to assess the pore connectivity of PC systems using conventional methods such as mercury intrusion porosimetry and scanning electron microscope (SEM), these techniques cannot assess the connectivity of pores directly. This is particularly true for AASC systems, which are reported to have higher proportions of mesopores than PC systems [4] and poorer permeation properties for a given compressive strength grade [5]. Accurate interpretation of these observations requires further study on pore network connectivity (tortuosity) of AASC systems. The first ever three-dimensional pore structure characterisation of alkali-activated binders was carried out by Provis *et al* [6]. Based on X-ray micro-tomography, much lower tortuosity was reported for AASC systems compared to PC controls after 28 days, while these observations

did not include assessment of microstructural development during the hydration process.

In this work, the main objective is to propose a simple method to investigate the pore structure development of AASC systems.

2. GOVERNING EQUATION

The electrical conductivity of cement-based materials is a function of several factors, including the geometrical configuration of electrodes, connectivity of capillary pores, level of pore saturation, and concentration and mobility of ions in the pore water. Since the electrical conductivity of solid and void phases are several orders of magnitude lower than liquid phases, the former two are generally considered as non-conductive. Therefore, an equation describing the electrical conductivity of hardened cementitious materials is [7]:

$$C_t = C_0 \phi \beta \quad \text{Eq (1)}$$

where C_t is the bulk conductivity of a mortar specimen (S/m), C_0 is the conductivity of pore solution (S/m), ø is the liquid-filled porosity (%), β is the pore connectivity factor. Experimentally, Eq. (1) can be applied to estimate the connectivity factor, provided the bulk conductivity of a mortar specimen, the conductivity of pore solution and the liquid-filled porosity are also determined.

3. MATERIALS AND METHODS

3.1 Raw materials

Ground granulated blast furnace slag (GGBFS) provided by Chongqing Iron and Steel Company was initially ground for 40 mins in a ball mill, after which its specific area and density were measured. PC confirming to GB175-2007 was used to manufacture comparison specimens. Activator for the AASC mixes was liquid sodium silicate with a pre-specified modulus 1.2 defined as the mole ratio of SiO_2 to Na_2O. A constant alkaline concentration of 5% by wt. of GGFBS (Na_2O equivalent) was used in this study. Medium graded natural sand with a fineness modulus of 2.60 was used as fine aggregate.

3.2 Sample preparation

The mortar specimens were formulated with a sand to binder ratio of 3:1 by mass. Mortar specimens prepared included 40 mm cubes and 40×40×160 mm prisms, while paste was cast in cylinder moulds with diameter 40 mm and height 100 mm. All specimens were de-moulded after 24 hours and subsequently cured in water at a constant temperature of 20±2 °C until testing. The 40 mm cubic mortar specimens were used for measuring bulk electrical conductivity. The paste specimens were used to extract pore solution for conductivity, accessible porosity and microstructural feature analysis.

3.3 Test methods

Compressive and flexural strengths were determined according to the Chinese National Standard GB/T 17671-1999. Resistivity of mortar samples was tested using a two-point uniaxial method with an LCR bridge. Accessible porosity was assessed using Le Chatelier Flask's method. Pore solutions from AASC and PC paste samples were extracted using equipment used in conjunction with a compression machine. Further details of this experimental method are as described by Vollpracht *et al* [8]. SEM and X-ray microtomography were applied as an aid to validate the conclusions derived from electrical responses.

4. RESULTS AND DISCUSSION

4.1 Mechanical and electrical properties

Mechanical properties of the AASC and PC mortar specimens at different ages are plotted in **Fig. 1**. As expected, both compressive and flexural strength increases with age for both materials types, albeit at different rates. More specifically, AASC mortars shows a rapid compressive strength increase for the first 14 days, yielding pronounced differences between the two binder types. This can be attributed to fast rates of chemical reaction between alkali-activator and slag particles [9].

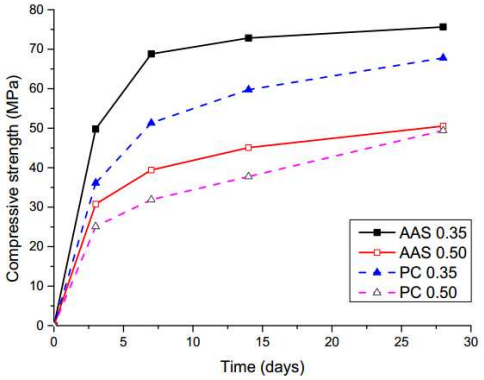

Figure 1. Compressive strength of AASC and PC

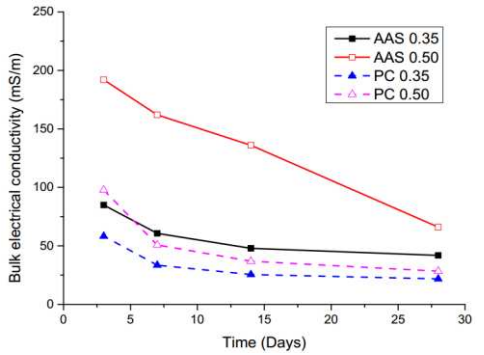

Figure 2. Bulk electrical conductivity of mortar specimens

Electrical conductivity results for the mortar specimens considered are presented in **Fig. 2**. As expected, bulk electrical conductivity of both the AASC and PC mixes exhibited a decreasing trend with age, especially over the first 7 days. Differences between the AASC and PC mixes were more pronounced for the 0.50 w/b ratio mixes. This is because more liquid is present in a given sample as its w/b ratio increases, resulting in higher conductivity. In the case of AASC mixes, however, increase in w/b ratio decreases the concentration of alkali-ions present provided the total alkali content is kept constant. As such, the degree of GGBFS hydration decreases with increasing liquid phases. Because of this difference from conventional PC mixes, AASC mixes are more sensitive to w/b ratio.

4.2 Accessible porosity and pore solution conductivity

Figure 3 presents values of accessible porosity, which for both the AASC and PC mortar mixes generally decreased with age and w/b ratio as expected. Meanwhile, the PC mortar mixes were more porous than the AASC mixes. This finding correlates with previous work, which from mercury intrusion porosimetry analysis showed that AASC-based materials contain fewer pores with diameters greater than 100 nm than PC materials, regardless of water to binder ratio. Similar trends are reported elsewhere in the literature [4,6].

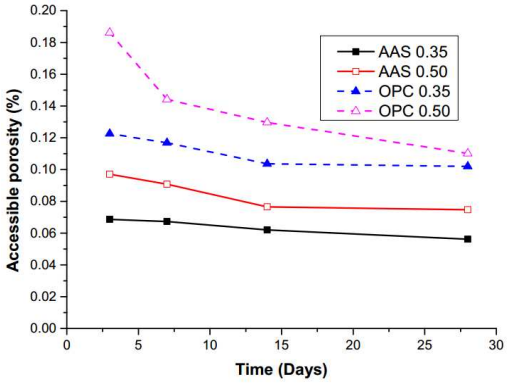

Figure 3. Accessible porosity of mortar specimens

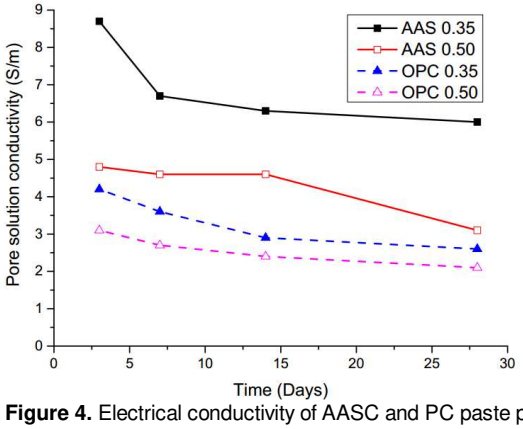

Figure 4. Electrical conductivity of AASC and PC paste pore solutions

The electrical conductivity of AASC and PC pore solutions are given in **Fig. 4**, which similarly shows decreasing trends as a function of time. In this instance, however, values for the AASC mortar mixes were higher than for the PC controls. This was particularly apparent at a w/b of 0.35, where the AASC mix exhibited markedly higher pore solution conductivity values, especially at early ages. The differences between mixes noted in **Fig. 4** are similar to those reported and previous research [10].

4.3 Pore connectivity

Figure 5 shows the estimated connectivity factor of AASC and PC mixes at different age. The influence of w/b ratio was apparent for the PC mortar mixes, with connectivity factor values for the 0.50 w/b mixes on average 57% higher than the 0.35 w/b ratios across the range of ages considered. A similar but much more pronounced effect was clear for the AASC mortar mixes. In this instance, the 0.50 w/b mix results were on average 180% higher that corresponding 0.35 w/b specimens, indicating AASC's sensitivity to w/b ratio changes. In terms of relative performance, the results highlight that equivalent performance is not achieved by AASC and PC mixes with equal w/b ratios.

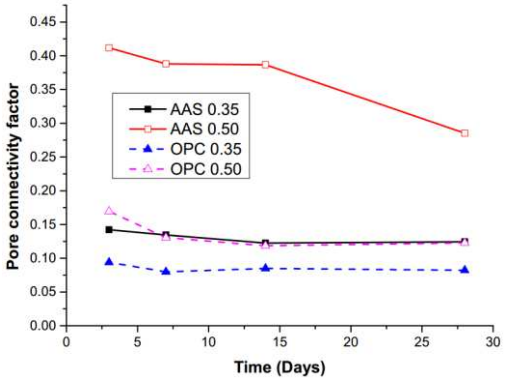

Figure 5. Pore connectivity factors for AASC and PC mortars as a function of time

4.4 SEM and X-ray computed tomography analysis

To further investigate the microstructure of the AASC and PC materials and verify the findings obtained from the electrical response-based pore connectivity results, SEM and X-ray computed tomography techniques were used. Shown in **Fig. 6** are SEM images of AASC and PC paste specimens. Clearly AASC paste hydration products have fewer topographical features and appear much denser that PC paste hydration products. A further difference is that AASC hydration products are connected by clearly defined cracks. Cracks in AASC-paste caused by shrinkage and low water-bonding capacity have been identified and discussed in previous related research [1,5] and are reported to contribute to high connectivity factors and provide potential pathways for aggressive substance permeation.

The 3D microstructure of porous materials pore structure reconstructions were developed for the AASC and PC paste samples using X-ray computed tomography is shown in **Fig. 7**. It is evident from these images that reconstructed PC paste solid phases are denser than those for AASC paste and that the pore network in the former appears to be disconnected. These finding are in line with previous μCT work concerning AASC and PC [6,11], which reported that the segmented porosity of PC paste is approximately 0.20, as opposed to 0.26 for AASC samples.

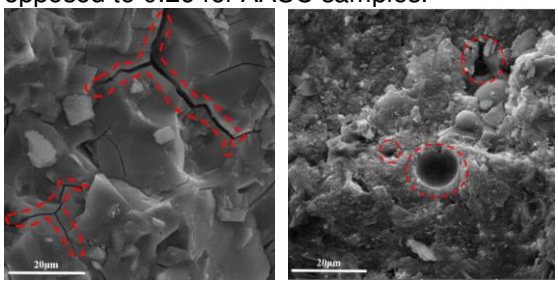

AASC PC

Figure 6. SEM images of AASC and PC paste with water to binder ratio of 0.35 at 28 days

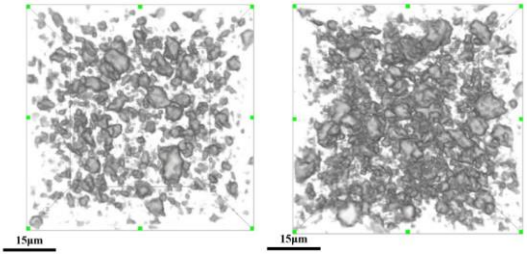

Figure 7. SEM images of AASC and PC paste with water to binder ratio of 0.35 at 28 days

5. CONCLUSIONS

Preliminary findings from the work reported here suggest that measurement of electrical response, in conjunction with porosity and pore solution data and the application of Archie's law, offers a promising route for characterising the pore structure development of AASC materials. The approach presented may circumvent experimental difficulties of measuring pore connectivity in the field and be suitable for assessing influences of time and external factors on AASC material performance changes.

ACKNOWLEDGEMENT

The experiments described in this paper were carried out in Chongqing University and Shenzhen University. The authors acknowledge these institutions for providing facilities and the financial support provided by National Natural Science Foundation of China (NO. 51408078), Open funds from Shenzhen University and State Key Laboratory of High Performance Civil Engineering Materials. Supports provided by University of Leeds are also highly appreciated.

REFERENCES

[1] Juenger M C G, Winnefeld F, Provis J L, Ideker J H. Advances in alternative cementitious binders. Cement and Concrete Research, 2011, 41(12): 1232-1243.

[2] Turner L K, Collins F G. Carbon dioxide equivalent (CO_2-e) emissions: a comparison between geopolymer and OPC cement concrete. Construction and Building Materials, 2013, 43: 125-130.

[3] Deventer J S J V, Provis J L, Duxson P. Technical and commercial progress in the adoption of geopolymer cement. Minerals Engineering, 2012, 29(3): 89-104.

[4] Collins F, Sanjayan J G. Effect of pore size distribution on drying shrinking of alkali-activated slag concrete. Cement and Concrete Research, 2000, 30(9): 1401-1406.

[5] Yang K, Yang C, Magee B, Magee B, Nanukuttan S, Ye J. Establishment of a preconditioning regime for air permeability and sorptivity of alkali-activated slag concrete. Cement and Concrete Composites, 2016, 73: 19-28.

[6] Provis J L, Myers R J, White C E, Rose V, Deventer J S J V. X-ray microtomography shows pore structure and tortuosity in alkali-activated binders. Cement and Concrete Research, 2012, 42(6): 855-864.

[7] Rajabipour F, Weiss J. Electrical conductivity of drying cement paste. Materials and Structures, 2007, 40(10): 1143-1160.

[8] Vollpracht A, Lothenbach B, Snellings R, Haufe J. The pore solution of blended

cements: a review. Materials and Structures, 2016, 49(8):3341-3367.
[9] Ding Y, Dai J G, Shi C J. Mechanical properties of alkali-activated concrete: A state-of-the-art review. Construction and Building Materials, 2016, 127:68-79.
[10] Ma Q, Nanukuttan S V, Basheer P A M, Bai Y, Yang C. Chloride transport and the resulting corrosion of steel bars in alkali activated slag concretes. Materials and Structures, 2016, 49(9): 3663-3677.
[11] Bernardes E E, Carrasco E V M, Vasconcelos W L, Magalhães A G. X-ray microtomography (μ-CT) to analyze the pore structure of a Portland cement composite based on the selection of different regions of interest. Construction and Building Materials, 2015, 95:703-709.